

LETTERS

Significant decadal-scale impact of volcanic eruptions on sea level and ocean heat content

John A. Church^{1,2}, Neil J. White^{1,2} & Julie M. Arblaster^{3,4}

Ocean thermal expansion contributes significantly to sea-level variability and rise¹. However, observed decadal variability in ocean heat content^{2,3} and sea level⁴ has not been reproduced well in climate models⁵. Aerosols injected into the stratosphere during volcanic eruptions scatter incoming solar radiation, and cause a rapid cooling of the atmosphere^{6,7} and a reduction in rainfall^{6,8,9}, as well as other changes in the climate system⁷. Here we use observations of ocean heat content^{2,3} and a set of climate simulations to show that large volcanic eruptions result in rapid reductions in ocean heat content and global mean sea level. For the Mt Pinatubo eruption, we estimate a reduction in ocean heat content of about 3×10^{22} J and a global sea-level fall of about 5 mm. Over the three years following such an eruption, we estimate a decrease in evaporation of up to 0.1 mm d^{-1} , comparable to observed changes in mean land precipitation^{6,8,9}. The recovery of sea level following the Mt Pinatubo eruption in 1991 explains about half of the difference between the long-term rate of sea-level rise⁴ of 1.8 mm yr^{-1} (for 1950–2000), and the higher rate estimated for the more recent period where satellite altimeter data are available (1993–2000)^{4,10}.

Coupled climate models show better agreement with observations on both annual and decadal timescales when volcanic forcing is included^{11–13}. Volcanic eruptions also lead to changes in ocean heat content^{14,15} but, to date, there has been little focus on their impact on sea level, other than suggestions that they may be responsible for a component of observed decadal variability⁴.

In order to isolate the volcanic signal, we use a subset of the climate simulations completed with the Parallel Climate Model (PCM¹⁶). The PCM has an atmospheric resolution of about 2.8° by 2.8° with 18 levels in the vertical and an ocean resolution of $2/3^\circ$ to $1/2^\circ$ and 32 levels¹⁷. We use two three-member ensembles started from different points in the control run. The first ensemble has time-varying volcanic, solar, greenhouse gases, tropospheric (non-volcanic) sulphates and ozone ('VSGSuOz') forcing. The second has 'SGSuOz' forcing, with the volcanic component omitted. We also use the control simulation, in which the forcing is constant. The zonally averaged volcanic forcing¹² (indicated by atmospheric optical depth in the figures) used here for the period 1890–2000 (that is, starting after the large Krakatoa eruption of 1883) was derived in a consistent way based on the total amount of sulphate released and consideration of the seasonally varying stratospheric transport and decay.

We calculated the change in global mean sea level (GMSL), relative to the control run, resulting from ocean thermal expansion from 1890 to 2000 from monthly-averaged temperatures and salinities. For the SGSuOz (VSGSuOz) simulations, there was an increase in GMSL of about 43 mm (37 mm) over the 110 yr time span (Fig. 1a). There were two large volcanic eruptions before 1915, then a relatively quiescent period followed by a sequence of major eruptions starting in 1963, of which the three largest were Mt Agung (Indonesia, 1963),

El Chichon (Mexico, 1982) and Mt Pinatubo (Philippines, 1991). Following each eruption there was a fall in GMSL of several millimetres and an abrupt cooling of the ocean, typically within a year.

The volcanic GMSL (full ocean depth) and global ocean heat content (GOHC, upper 300 m only) signal was identified by subtracting results from pairs of simulations with and without volcanic forcing and forming the ensemble average of these differences (Fig. 1b, c). There is uncorrelated variability in the individual ensemble members associated with mismatches in signals from climate variability such as El Niño/Southern Oscillation (ENSO), but the volcanic signal is clear. GMSL and GOHC fall by about 5 mm

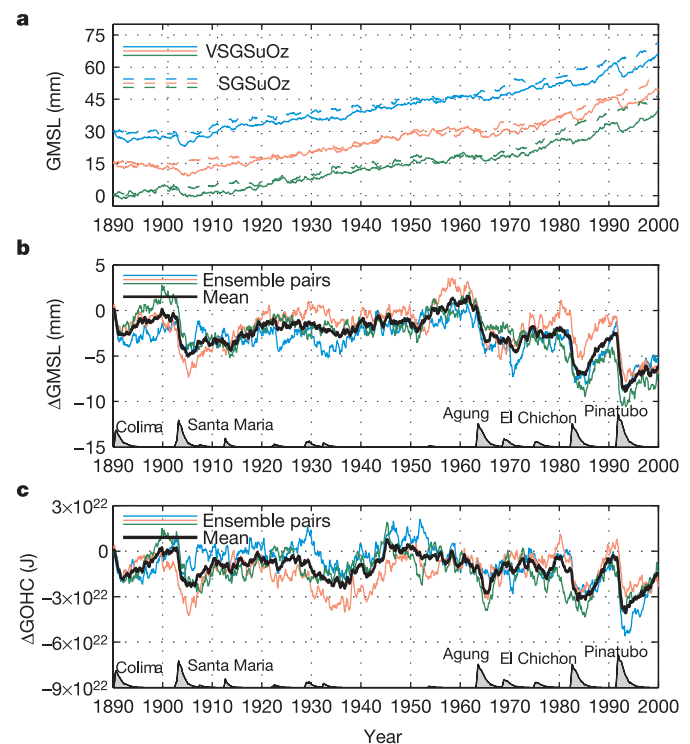


Figure 1 Changes in global mean sea level (GMSL) and global ocean heat content (GOHC) in the PCM simulations. **a**, Three pairs of simulations of full depth GMSL with time-varying volcanic, solar, greenhouse gases, sulphates and ozone ('VSGSuOz') forcing and the corresponding simulations without the volcanic forcing ('SGSuOz') are shown respectively by the solid and dashed lines. The differences between the pairs for GMSL (Δ GMSL; **b**) and GOHC (upper 300 m only) (Δ GOHC; **c**) are the coloured lines and the ensemble average is the bold black line. The global average optical depth (stratospheric optical depth at $0.5 \mu\text{m}$; ref. 12) is also shown (thin black line at bottom; arbitrary scale).

¹CSIRO Marine and Atmospheric Research, GPO Box 1538, ²Antarctic Climate and Ecosystems Cooperative Research Centre, Hobart, Tasmania 7001, Australia. ³National Center for Atmospheric Research, Boulder, Colorado 80307-3000, USA. ⁴Bureau of Meteorology Research Centre, Melbourne, Victoria 3001, Australia.

and 3×10^{22} J (the largest response follows the Mt Pinatubo eruption) and then rise over the following decade or more. Smaller eruptions followed the 1903 Santa Maria and the 1963 Mt Agung eruptions, and in these cases the recovery to pre-eruption levels took in excess of 15 yr. For the Mt Pinatubo eruption, the recovery was not complete at the end of the simulations in 2000. Over 1890 to 2000, the volcanic forcing leads to a reduction of about 6 mm in GMSL, most of which occurs from 1960 to 2000. This reduction offsets part of the acceleration in sea-level rise in the latter part of the twentieth century in the SGSuOz simulations.

We compare two estimates (Levitus *et al.*² and Ishii *et al.*³, updated 2005) of yearly GOHC and the associated thermal expansion component of sea level available after 1955 with the model results. We focus on the upper 300 m principally because of the better coverage of ocean data in this depth range, and because full depth and upper 300 m heat content (and sea-level) time series in the model are well correlated (for example, the correlation is 0.86 for sea level) and the variability of the pairs of time series are virtually the same magnitude. Despite this upper ocean focus, the major limitation of these ocean products is the lack of global coverage¹⁸ and reliable error estimates. The two estimates of observed GOHC and GMSL are well correlated (both above 0.8) and show a similar decrease following major volcanic eruptions. For the observations, it is not possible (as it is in the model simulations) to separate the response to the volcanic forcing from other external forcing, and the observations contain contributions from natural climate variability (for example, ENSO events) that may occur at different times to the model's internal variability. Despite the uncertainties in the volcanic forcing and the incomplete ocean database, the detrended GMSL and GOHC time series (Fig. 2) are correlated with the detrended model results, 0.59 (0.59) and 0.49 (0.44), respectively for the Levitus² (Ishii³) data sets. These post-eruption drops in sea level agree qualitatively with the observed (tide-gauge based⁴) GMSL record.

For the Mt Pinatubo eruption, for which there are better observations of stratospheric aerosols and ocean heat content, the observed GMSL and GOHC fall by about 5 mm and 3×10^{22} J, similar to the model ensemble average. This agreement supports the validity of the stratospheric aerosol loading for the Mt Pinatubo eruption¹². The slow recovery towards pre-eruption values is slightly faster in the observations than in the model. The observations are also clearly affected by the 1997/98 ENSO event.

For the 1963 Mt Agung and the 1982 El Chichon eruptions, the magnitude of the observed signal is more than twice that of the model results. For the Mt Agung eruption, the stratospheric aerosol concentration used here¹² is only 20% larger in the (ocean-dominated) Southern Hemisphere than in the Northern Hemisphere, whereas other studies suggest that it should be a factor of three to eight larger¹². To test the sensitivity of the PCM results, we use three additional climate models that use volcanic forcing. These are the twentieth-century simulations (20C3M) of the NASA Goddard Institute for Space Studies (GISS-ER) model (nine-member ensemble), and the Centre for Climate System Research, University of Tokyo, high resolution model (MIROC3.2(hires), one ensemble member) and medium resolution model¹⁹ (MIROC3.2(medres), three-member ensemble). (Documentation of these models is available from <http://www-pcmdi.llnl.gov>.) As there are no comprehensive sets of simulations available to us for these additional models that allow the specific volcanic response to be isolated, we remove the long-term sea-level rise by subtracting a quadratic (the approximate expected response to increasing greenhouse gases) from the full model depth GMSL time series for all of the models, including the PCM. The residuals (Fig. 2c) will contain the interannual volcanic signal as well as other variability. For the PCM model, the residuals are very similar to the results obtained by differencing the volcanic-non volcanic simulations. The response of all of the models is very similar (correlations between 0.7 and 0.9), and the GISS/MIROC correlations (which both use an update of the Sato *et al.*²⁰ volcanic

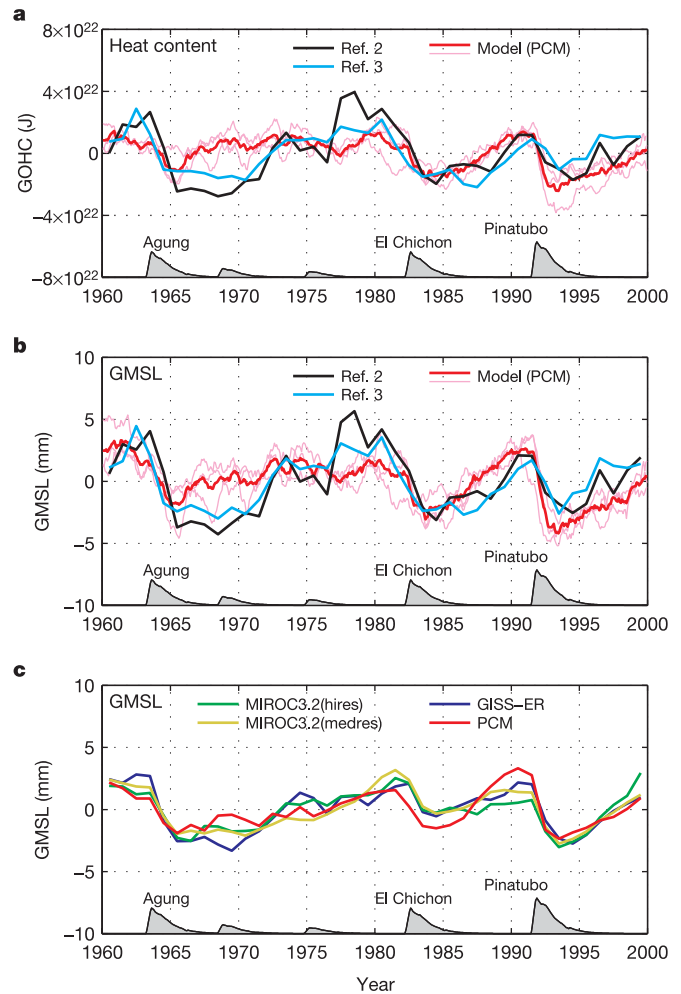


Figure 2 | Observed and modelled GOHC and GMSL for the period 1960–2000. The response to volcanic forcing, as indicated by the differences between the pairs of PCM simulations for GOHC (**a**) and the GMSL (**b**) is shown for the ensemble mean (bold line) and the three ensemble members (light lines). The observational estimates^{2,3} of GOHC and GMSL are shown by the black and blue bold lines. For **a** and **b**, all results are for the upper 300 m only and have been detrended over the period 1960–2000. **c**, The ensemble mean (full depth) GMSL for the GISS-ER, MIROC3.2(hires), MIROC3.2(medres) and the PCM models (after subtracting a quadratic) are shown.

forcing) are above 0.85. The GISS-ER model has the largest response, particularly for the Mt Agung eruption, but still smaller than the observed response. The remaining discrepancies between the observations and the model results may be due to the inadequate ocean database (particularly large gaps in the Southern Hemisphere coverage¹⁸) used for determining observed GOHC and GMSL, as well as uncertainties in the volcanic forcing and climate model sensitivity.

To better understand the processes involved, we focus on the Mt Pinatubo eruption (June 1991) because of its stronger radiative forcing and the better observations available. The primary driver of the fall in sea-surface temperature, GMSL and GOHC in the PCM is the rapid reduction in net solar flux at the ocean surface (Fig. 3a) of up to 6 W m^{-2} in late 1991. By early 1994, the net solar flux had virtually recovered to pre-eruption values, even though the optical depth from the volcanic aerosols had not yet recovered. The net shortwave forcing recovers to pre-eruption values faster than the volcanic optical depth, perhaps as a result of reduced cloud cover, as found in earlier model studies⁶. In the global average, the fall in the model sea surface temperature is about $0.4 \text{ }^\circ\text{C}$ and almost recovers to pre-eruption values in 1995, whereas observations²¹ show a smaller

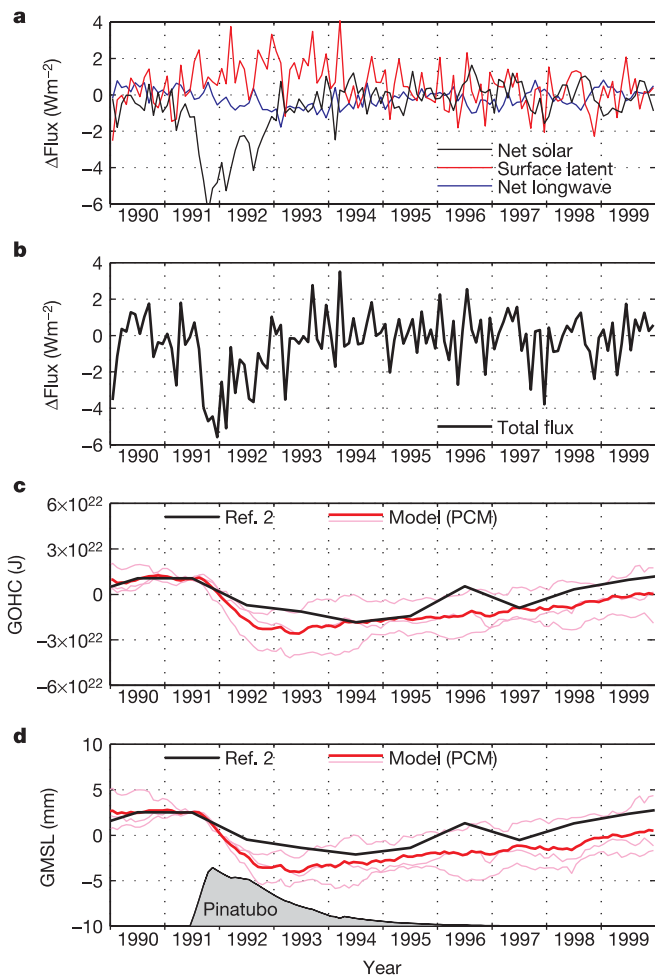


Figure 3 Ocean heat budget anomalies associated with the Mt Pinatubo eruption. **a**, The net solar (black), latent heat (red) and net long-wave (blue) heat fluxes. **b**, The total surface heat flux. Positive (negative) fluxes are a warming (cooling) of the ocean, and the fluxes are the averages of the differences between the three ensemble pairs. **c**, The modelled and observed² GOHC. **d**, The modelled and observed² GMSL. For **c** and **d**, the three ensemble pair differences between the models with and without volcanic forcing are shown as light lines, and the ensemble average bold, and are for the upper 300 m only.

fall (about 0.3°C) and a faster recovery. In both observed and modelled sea surface temperature, the cooling occurs over a band from about 50°S to 60°N , with maximum cooling at mid-latitudes during the Southern Hemisphere summer of 1991/1992 and the Northern Hemisphere summer of 1992. The maximum cooling of both hemispheres in the summer is probably a result of shallow mixed layers at this time of year, which respond more rapidly to a given heat flux change. Sea-ice feedbacks⁶ may also be a factor.

The latent heat flux anomaly (a warming of the ocean of 2 W m^{-2} peaking in early 1993, Fig. 3a) corresponds to reduced evaporation of about 0.1 mm d^{-1} , agreeing with observed land mean precipitation reductions following volcanic eruptions^{8,9}. The maximum in the latent heat flux anomaly occurs at about the same time as the minimum of sea surface temperature and 12 months after the maximum reduction in the shortwave flux. There is also a smaller ocean cooling from the net longwave flux. The ocean cools rapidly as a result of the reduction in the total heat flux of about 5 W m^{-2} . This total flux is consistent with the observed reduction in the net forcing of the climate system between 40°N and 40°S (land and ocean)²² of 4.3 W m^{-2} . The cooling peaks in late 1991, returning to almost zero by mid-1993, then the ocean slowly warms (Fig. 3b). As a result, the

GOHC and GMSL (upper 300 m only; Fig. 3c, d) fall rapidly for 12 to 18 months following the eruption, with a slower recovery, which was not complete by 2000. The model results for the full ocean depth suggest that sea level recovers more rapidly than heat content, perhaps as a result of more rapid ocean turnover times in low latitudes where the thermal expansion coefficient is larger. In cooler, high-latitude waters with smaller thermal expansion coefficients, the heat anomalies may have been advected into the main thermocline where they would remain for decades, as found in simulations that include the larger Krakatoa (1883) and Tambora (1815) eruptions (ref. 23, and J.M. Gregory, J.A. Lowe and S.F.B. Tett, manuscript in preparation).

Quantifying the impacts of volcanic eruptions is important to understanding climate and GMSL variability, and there are important consequences for interpretation of the observational record. The rate of sea-level rise for the modern satellite altimeter era (3.2 mm yr^{-1} for 1993–2000)^{4,10} is significantly larger than the 1950–2000 rate⁴ of 1.8 mm yr^{-1} . The PCM model results indicate that the rate of sea-level rise calculated for 1993–2000 should be about 0.5 mm yr^{-1} higher than the average rate of sea-level rise over the preceding four decades, because of the recovery of sea level from the effects of the Mt Pinatubo eruption. This recovery, together with recent increases in glacier and ice sheet contributions^{24–28} (greater than 0.5 mm yr^{-1}), explains much of the difference between the 1950–2000 and 1993–2000 estimates of sea-level rise.

Received 8 June; accepted 27 September 2005.

- Church, J. A. *et al.* in *Climate Change 2001: The Scientific Basis* (ed. Houghton, J. T.) 639–694 (Cambridge Univ. Press, Cambridge, 2001).
- Levitus, S., Antonov, J. I. & Boyer, T. P. Warming of the World Ocean, 1955–2003. *Geophys. Res. Lett.* **32**, L02604 (2005) doi:10.1029/2004GL021592.
- Ishii, M., Kimono, M. & Kachi, M. Historical ocean subsurface temperature analysis with error estimates. *Mon. Weath. Rev.* **131**, 51–73 (2003).
- Church, J. A., White, N. J., Coleman, R., Lambeck, K. & Mitrovica, J. X. Estimates of the regional distribution of sea-level rise over the 1950 to 2000 period. *J. Clim.* **17**, 2609–2625 (2004).
- Gregory, J. M. *et al.* Comparison of results from several AOGCMs for global and regional sea-level change 1900–2100. *Clim. Dyn.* **18**, 225–240 (2001).
- Robock, A. & Liu, Y. The volcanic signal in Goddard Institute for Space Studies three-dimensional model simulations. *J. Clim.* **7**, 44–55 (1994).
- Robock, A. Volcanic eruptions and climate. *Rev. Geophys.* **38**, 191–219 (2000).
- Gillett, N. P., Weaver, A. J., Zwiers, F. W. & Wehner, M. F. Detection of volcanic influence on global precipitation. *Geophys. Res. Lett.* **31**, L12217, doi:10.1029/2004GL020044 (2004).
- Lambert, F., Stott, P. A., Allen, M. R. & Palmer, M. A. Detection and attribution of changes in 20th century land precipitation. *Geophys. Res. Lett.* **31**, L10203, doi:10.1029/2004GL019545 (2004).
- Leuliette, E. W., Nerem, R. S. & Mitchum, G. T. Calibration of TOPEX/Poseidon and Jason altimeter data to construct a continuous record of mean sea level change. *Mar. Geod.* **27**, 79–94 (2004).
- Stott, P. A. *et al.* External control of 20th century temperature by natural and anthropogenic forcings. *Science* **290**, 2133–2137 (2000).
- Ammann, C. M., Meehl, G. A. & Washington, W. M. A monthly and latitudinally varying volcanic forcing dataset in simulations of the 20th century climate. *Geophys. Res. Lett.* **30**, 16257, doi:10.1029/2003GL016875 (2003).
- Broccoli, A. J. *et al.* Twentieth-century temperature and precipitation trends in ensemble climate simulations including natural and anthropogenic forcing. *J. Geophys. Res.* **108**, 4798, doi:10.1029/2003JD003812 (2003).
- Sun, S. & Hansen, J. E. Climate simulations for 1951–2050 with a coupled atmosphere-ocean model. *J. Clim.* **16**, 2807–2826 (2003).
- Hansen, J. E. *et al.* Earth's energy imbalance; confirmation and implications. *Science* **308**, 1431–1435 (2005).
- Meehl, G. A. *et al.* Combinations of natural and anthropogenic forcings in 20th century climate. *J. Clim.* **17**, 3721–3727 (2004).
- Washington, W. M. *et al.* Parallel climate model (PCM) control and transient simulations. *Clim. Dyn.* **16**, 755–774 (2000).
- Gregory, J. M., Banks, H. T., Stott, P. A., Lowe, J. A. & Palmer, M. D. Simulated and observed decadal variability in ocean heat content. *Geophys. Res. Lett.* **31**, L15312, doi:10.1029/2004GL020258 (2004).
- Nozawa, T., Nagashima, T., Shiogama, H. & Crooks, S. A. Detecting natural influence on surface air temperatures change in the early twentieth century. *Geophys. Res. Lett.* (in the press).
- Sato, M., Hansen, J. E., McCormick, M. P. & Pollack, J. B. Stratospheric aerosol optical depths, 1850–1990. *J. Geophys. Res.* **98**, 22987–22994 (1993).

21. Rayner, N. *et al.* Global analyses of sea surface temperature, sea ice, and night marine air temperature since the late nineteenth century. *J. Geophys. Res.* **108**, 4407, doi:10.1029/2002JD002670 (2003).
22. Minnis, P. *et al.* Radiative climate forcing by the Mount Pinatubo eruption. *Science* **259**, 1411–1415 (1993).
23. Delworth, T. L., Ramaswamy, V. & Stenchikov, G. L. The impact of aerosols on simulated ocean temperature, heat content, and sea level in the 20th century. *Geophys. Res. Lett.* (submitted).
24. Arendt, A. A., Echelmeyer, K. A., Harrison, W. D., Lingle, C. S. & Valentine, V. B. Rapid wastage of Alaska glaciers and their contributions to rising sea level. *Science* **297**, 382–386 (2002).
25. Thomas, R. *et al.* Accelerated sea-level rise from West Antarctica. *Science* **306**, 255–258 (2004).
26. Rignot, E. *et al.* Accelerated ice discharge from the Antarctic Peninsula following the collapse of the Larsen B ice shelf. *Geophys. Res. Lett.* **31**, 118401, doi:10.1029/2004GL020697 (2004).
27. Rignot, E., Rivera, A. & Casassa, G. Contribution of the Patagonia Icefields of South America to sea level rise. *Science* **302**, 434–437 (2003).
28. Kraybill, W. *et al.* Greenland Ice Sheet: Increased coastal thinning. *Geophys. Res. Lett.* **31**, L24402, doi:10.1029/2004GL021533 (2004).

Acknowledgements This paper is a contribution to the CSIRO Climate Change Research Program. This work was supported by the Australian Government's Cooperative Research Centres Programme through the Antarctic Climate and Ecosystems Cooperative Research Centre (ACE CRC). Portions of this study were supported by the Office of Biological and Environmental Research, US Department of Energy, as part of its Climate Change Prediction Program, and by the National Center for Atmospheric Research. The National Center for Atmospheric Research is sponsored by the National Science Foundation. We acknowledge the international modelling groups for providing their data for analysis, the Program for Climate Model Diagnosis and Intercomparison (PCMDI) for collecting and archiving the model data, the JSC/CLIVAR Working Group on Coupled Modelling (WGCM) and their Coupled Model Intercomparison Project (CMIP) and Climate Simulation Panel for organizing the model data analysis activity, and the IPCC WG1 TSU for technical support. The IPCC Data Archive at Lawrence Livermore National Laboratory is supported by the Office of Science, US Department of Energy. We thank T. Wigley for comments and insight.

Author Information Reprints and permissions information is available at npg.nature.com/reprintsandpermissions. The authors declare no competing financial interests. Correspondence and requests for materials should be addressed to J.A.C. (John.Church@csiro.au).